

As the two-dimensional electron density increases, the simple picture with two persistent exciton and trion lines in the reflectivity and absorption spectra changes. To begin with, the strength of the exciton line drops with increasing electron density. Simultaneously, the trion line intensity grows. At a certain electron density, when the Fermi energy (1–3 meV) becomes of the same order of magnitude as the trion binding energy (3–5 meV) but remains significantly lower than the exciton binding energy (20–30 meV), the exciton line is absent from the spectrum. This picture is in conflict with the postulate that a loosely bound state (trion) must be destroyed by an electron gas (by means of screening or filling phase space) at lower electron densities than a tightly bound state (exciton).

Moreover, a rise in the electron density leads to an enhancement of the trion binding energy in proportion to the Fermi energy of a two-dimensional electron gas. This finding is paradoxically at variance with the current concept of screening (Fig. 4). However, this picture reverses with a rise in temperature (up to 35 K), when the trionic states are destroyed; in other words, the exciton line intensity increases, while the trion binding energy drops. This finding indicates that all anomalous phenomena should be attributed to trions rather than electrons.

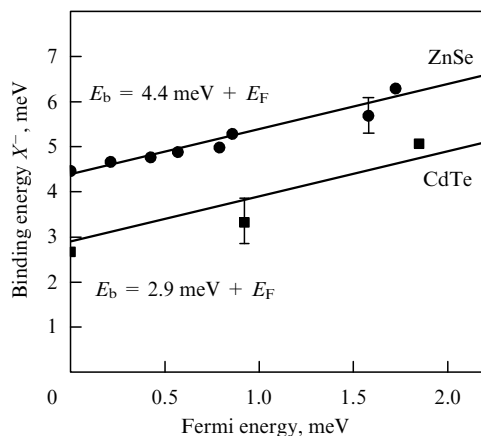


Figure 4. Dependence of the trion binding energy at the Fermi level of a two-dimensional electron gas for ZnSe- and CdTe-based quantum-well structures.

We explain such a behavior by the interaction between exciton and trion modes. The trion binding energy being low compared with the exciton binding energy and close to the uniform and nonuniform exciton broadening, the excitonic and trionic states may be regarded as having similar energies. Therefore, an exciton is readily converted to a trion when it takes up an additional electron. Conversely, a trion becomes an exciton after the loss of an electron. If this process is a coherent one, the modes intermix. In this case, exciton and trion are not independent excitations but should be considered as mixed exciton–trion modes. Such intermingling of exciton and trion excitations becomes more conspicuous with growing electron density and manifests itself as the redistribution of exciton and trion oscillator strengths and also as an increasing energy gap between these two lines.

We have developed a theory of such mixed exciton–trion excitations which agrees both qualitatively and quantitatively with experimental findings.

References

1. Kheng K et al. *Phys. Rev. Lett.* **71** 1752 (1993)
2. Yakovlev D R et al. *Phys. Rev. Lett.* **79** 3974 (1997)
3. Astakhov G V et al. *Phys. Rev. B* **60** R8485 (1999)
4. Yakovlev D R et al., in *Nanostructures: Physics and Technology (Seventh Int. Symp., St. Petersburg, Russia, 1999)* (St. Petersburg, 1999) p. 393
5. Wittaker D M, Shields A J *Phys. Rev. B* **56** 15185 (1997)
6. Kochereshko V P et al., in *Proc. of 23th Int. Conf. on the Physics of Semiconductors* (Berlin, Germany, 1996) p. 1943
7. Kochereshko V P et al. *Superlattices Microstruct.* **21** 269 (1998)
8. Kochereshko V P et al. *J. Cryst. Growth* **184/185** 826 (1998)

PACS numbers: 79.60.Jv, 85.30.Vw, **85.60.-q**

DOI: 10.1070/PU2000v043n03ABEH000703

Optical properties of strained $\text{Si}_{1-x}\text{Ge}_x$ and $\text{Si}_{1-x-y}\text{Ge}_x\text{C}_y$ heterostructures

Z F Krasil'nik, A V Novikov

1. Introduction

Recent progress in studies of silicon-based low-dimensional structures has given rise to a new field of research known as Si-based optoelectronics. Silicon and germanium are nondirect-gap materials, in which radiative recombination processes are hampered. However, low-dimensional structures based on these elements may be expected to show a number of previously unknown light emission characteristics.

On-going studies of novel mechanisms of effective photoluminescence from silicon are proceeding along several lines. One is focused on porous silicon structures and silicon nanoclusters embedded in a wider-bandgap host material. Using porous silicon structures, energies of photo- and electroluminescence in the range from 1 to 2.5 eV were obtained [4] and first integrated schemes were proposed in which light-emitting diodes are coupled to the control transistors [5].

Another line of research is concerned with silicon-based structures doped with rare-earth elements. Light emission by such structures is maintained by virtue of intracenter transitions which take place in rare-earth elements. For example, photo- and electroluminescence of erbium-doped silicon was reported to occur at 1.55 μm over a wide temperature range including room temperature [6]. The molecular-beam epitaxy (MBE) technology using sublimation sources proved very promising for the fabrication of heavily doped structures with a complex profile [7]. A recent publication describes laser generation with light pumping [8].

The third area of research gives priority to heterostructures with quantum wells and quantum dots based on direct-gap III–V semiconductors grown on a silicon substrate. Ref [9] reports the first results of a study of photoluminescence with a wavelength of 1.3 μm from a structure consisting of spontaneously formed quantum dots of InAs on a silicon substrate.

Finally, an important area of research is photoluminescence from $\text{Si}_{1-x}\text{Ge}_x$ and $\text{Si}_{1-x-y}\text{Ge}_x\text{C}_y$ nanostructures grown on a silicon substrate. Of special interest are the former structures with self-assembled nanoislands, in which intense luminescence near 1.55 μm was observed [10].

The present paper reports the results of a study on the growth of $\text{Si}_{1-x}\text{Ge}_x$ self-assembled nanoscale islands on

Si(100). It is in the first place devoted to the specific features of photoluminescence from nanoisland structures and the mechanisms of quasi-direct optical transitions in such structures. Along with the final results of the study, the paper discusses conceptual problems concerning direct radiative recombination in low-dimensional structures based on solid solutions of $\text{Si}_{1-x-y}\text{Ge}_x\text{C}_y$.

2. Growth and characteristics of $\text{Si}_{1-x}\text{Ge}_x$ nanoislands on Si(100)

The structures studied were grown by molecular-beam epitaxy on (100) silicon substrates at 550–700 °C. Silicon and germanium were evaporated using electron guns. First, a buffer silicon layer approximately 200 nm thick was grown on the substrate. A germanium layer was then deposited to a thickness equivalent to approximately 13 monolayers (ML). The structures thus obtained were used to measure island parameters by atomic-force and electron microscopy. For optical studies, the structures were covered with a 100-nm silicon layer.

The growth of germanium on a silicon substrate at 700 °C is fairly well described by the Stranski–Krastanov mechanism. In the general case, the heterogeneous interface layer between Si and Ge is stressed because of lattice mismatch due to a 4.2% difference between the lattice parameters of the heteropair. The pseudomorphic growth of the first 4–5 germanium ML (the wetting layer) is followed, in the course of further germanium deposition, by the formation of three-dimensional structures, so-called hut clusters [11] which are in fact small pyramidal well-faceted nanoislands with {105} planes as side faces.

Continuing deposition of germanium leads to a proportional increase in the linear dimensions of hut islands until they reach a certain critical volume (on the order of $3 \times 10^5 \text{ nm}^3$ under our growth conditions). Energetically favorable minimization of elastic stresses in islands of greater volume is attainable if their height to lateral dimension ratio exceeds that of hut clusters. Islands having volume greater than the critical one are dome-shaped and their lateral faces are oriented on planes {113} and {102} (dome islands) [12].

As the amount of deposited germanium continues to increase, the lateral dimensions of dome islands do not significantly change and they grow mainly in height. However, the height of such domes is also limited, which opens the possibility to obtain an array of uniformly-sized nanoscale structures after the transition from hut islands to dome islands is completed and the finite height of the latter is achieved. Under our experimental conditions, this occurred after the deposition of germanium sufficient to grow 11 ML. The dispersion of nanoisland dimensions did not exceed 10% at their mean height of 20 nm, lateral size of 100 nm, and surface density of about $3 \times 10^9 \text{ cm}^{-2}$ (Fig. 1).

Atomic-force and electron-microscopic studies have demonstrated that the total volume of dome islands is greater than the amount of the deposited germanium. This discrepancy can be accounted for by the bulk and surface diffusion of silicon into the growing islands. Such a diffusion was documented by Raman scattering and X-ray diffraction. Bulk diffusion occurred from the silicon buffer layer across the base of the islands. Surface diffusion resulted from the ‘perforation’ of the wetting layer on the island’s base perimeter, where elastic deformation forces were especially strong [3]. In the latter case, the silicon of the buffer layer

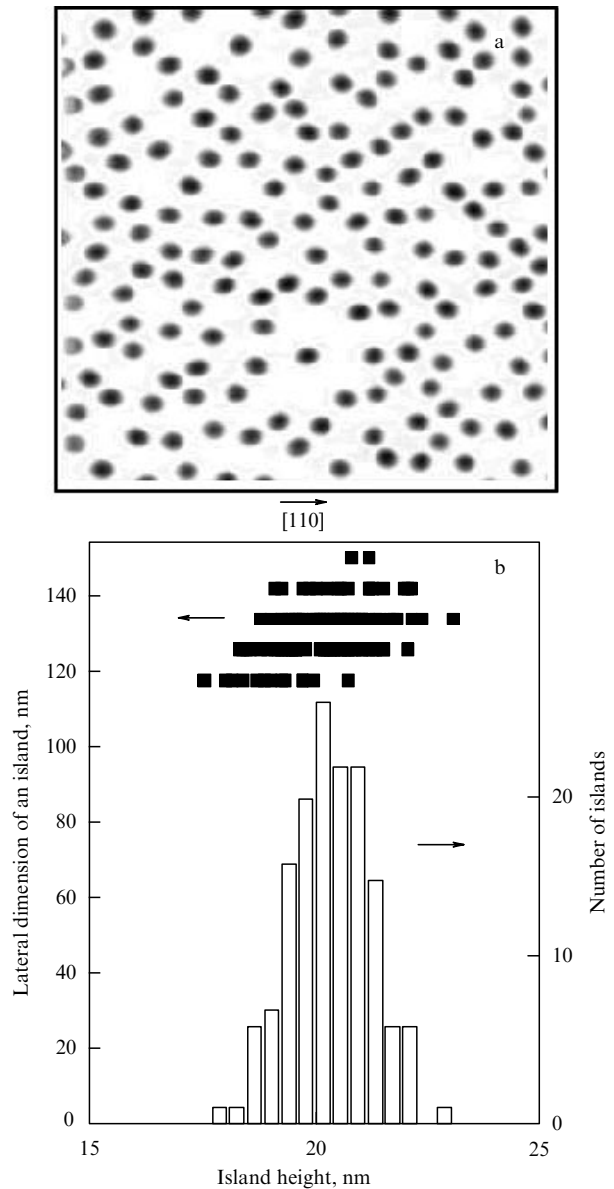


Figure 1. Inverted AFM image ($2.5 \times 2.5 \mu\text{m}^2$) of a sample containing 11 ML of Ge (a) and the results of its processing (b). Lateral dimension of an island is plotted against its height; histogram shows island distribution by heights.

diffused into the islands through their lateral facets. Our study has shown that silicon content in the nanoislands can be as high as 50%. This finding is used below to explain photoluminescence spectra (see below).

3. Radiative recombination in $\text{Si}_{1-x}\text{Ge}_x/\text{Si}$

Gaps in the conduction and valence bands at the heteroboundary between Si(100) and a solid $\text{Si}_{1-x}\text{Ge}_x$ solution are oriented in such a way that the potential wells for holes and electrons are localized in $\text{Si}_{1-x}\text{Ge}_x$ and silicon, respectively. Elastic deformation lifts the degeneracy of six equivalent Δ valleys. As a result, the bottom of the conduction band is formed by double-degenerate 2Δ valleys extended in the direction of the $\text{Si}_{1-x}\text{Ge}_x$ growth on Si(100). The silicon conduction band is shifted relative to the top of the $\text{Si}_{1-x}\text{Ge}_x$ -valence band in the same direction but in the momentum space.

If electrons inside silicon are for some reason are localized close to the heteroboundary (e.g., in the quantum well), it follows from the uncertainty relations that the electron's quasimomentum \mathbf{k} in the direction of the shift of the two bands relative each other may take arbitrary values, including $\mathbf{k} = 0$. Hence, the probability of direct electron transition from the conduction band of silicon to the valence band of $\text{Si}_{1-x}\text{Ge}_x$ in the momentum space with tunneling in the real space across the heteroboundary [1, 2] becomes nonzero.

The $\text{Si}_{1-x}\text{Ge}_x/\text{Si}$ heterostructures with self-assembled nanoislands are known to possess *p*-type conductivity with a bulk concentration of charge carriers of about $8 \times 10^{16} \text{ cm}^{-3}$. Holes from silicon accumulate in the potential wells of nanoislands, charging them positively. In the end, the holes driven by Coulomb repulsive forces must align along the island heteroboundaries. The positive charge of the islands causes bending of the bottom of the conduction band and creates a quantum well for electrons in silicon near the heterojunction (see inset in Fig. 2). This greatly facilitates the quasi-direct radiative recombination of silicon-supplied electrons with holes in nanoislands described above. Figure 2 illustrates the computation of the energy of such a transition depending on the composition of the solid solution.

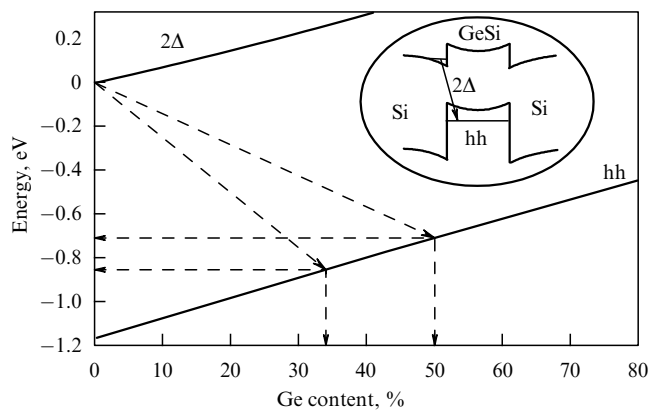


Figure 2. Position of the level of 2Δ electrons and heavy holes (hh) as a function of the germanium content in islands. The arrows show the energy region in which photoluminescence from the islands occurs and the range of island composition corresponding to these energies. The inset displays a schematic representation of quasi-direct optical transitions (see the main text).

Photoluminescence spectra taken at $T = 4.2 \text{ K}$ are shown in Fig. 3. The PL lines of islands are confined to the energy region from 0.7 to 0.85 eV, in agreement with the calculated radiative recombination for islands containing about 50% silicon. The long-wavelength wing of the photoluminescence line corresponds to energies lower than the width of the forbidden gap in bulk germanium, which can be explained only by the recombination of silicon-supplied electrons with holes in nanoislands, with tunneling across the heteroboundary.

Along with the signal from nanoislands in the energy region of the order of 1 eV, there are phonon and phononless peaks of photoluminescence from the two-dimensional wetting germanium layer 4–5 ML thick (Fig. 3). As germanium deposition continues to produce 7–10 ML, the photoluminescence from the two-dimensional wetting layer attenuates: the surface density of nanoislands increases and excitons photoexcited in the layer have enough time to diffuse

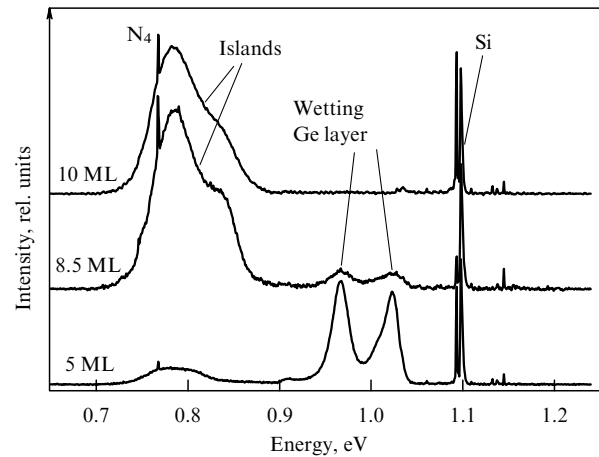


Figure 3. Dependence of the photoluminescence spectra of nanoisland structures on the thickness of the deposited germanium layer. Ge layer thickness (in ML) is shown above the corresponding spectral line; N_4 is the line produced by an impurity complex.

into the islands, where they participate in the recombination process.

The photoluminescence line remains wide enough (about 60 meV) even for a structure with nanoislands uniformly distributed by size. Irregular broadening of the line appears to be related to the inhomogeneous composition of the solid solution and nonuniform elastic stresses in nanoislands because of their irregular spacing in the growth plane. A shift of the photoluminescence line to the lower energy region with decreasing temperature can be attributed to a rise in the germanium content in the islands from 50 to 85% with a decrease in the growth temperature from 700 to 550 °C. In this experiment, the germanium content in the islands was monitored by X-ray diffraction and Raman measurements.

4. Heterostructures based on $\text{Si}_{1-x-y}\text{Ge}_x\text{C}_y$ solid solution

In $\text{SiGe}/\text{Si}(100)$ -based heterostructures, the potential barrier for electrons lies on a nanoisland and is extremely low, whereas the well for holes is sufficiently deep. For this reason, it is very difficult to localize electrons in silicon close to the heteroboundary with the islands. In other words, an overlap of electron and hole wave functions at the heteroboundary in the general case is too small to ensure an efficient direct-band recombination of electrons localized in silicon with tunneling across the heteroboundary. The addition of a small amount of carbon to the solid solution (to 3–5%) may lead to a substantial change in the structure of energy bands and even cause a transformation of type II to type I heteroboundary [13].

In the present study, band gaps for the heteroboundary between Si and $\text{Si}_{1-x-y}\text{Ge}_x\text{C}_y$ were theoretically deduced from the model proposed in Refs [14, 15]. In this model, valence band energies are computed on either side of the heteroboundary with respect to a certain absolute energy value, an analog of the vacuum level. Three major contributors to this energy are chemical, hydrostatic, and uniaxial deformations. Also, the model specially takes into account that the heteropair contains an alloy rather than an elementary semiconductor [16].

The results of calculations indicate that, in a $\text{Si}_{1-y}\text{C}_y$ binary solid solution grown on a silicon substrate, the wells for the holes and electrons are localized in the solution, while

the transition energy drops by 65 meV for each percent of carbon content (the decreased deformation and the chemical effect of carbon account for 46 and 19 meV, respectively) [13]. Band gaps are arranged in such a way that the well for electrons is deep while that for holes is shallow. The bottom of the conduction band in the well of the solid solution is formed by 2Δ electrons.

If the quantum well for electrons in $\text{Si}_{1-y}\text{C}_y$ adjoins that for holes in $\text{Si}_{1-x}\text{Ge}_x$, there is again a probability for quasi-direct radiative recombination between the electrons from $\text{Si}_{1-y}\text{C}_y$ and holes from $\text{Si}_{1-x}\text{Ge}_x$. In this case, the localization of 2Δ electrons is possible in a significantly smaller space than in the case of quantization of the bottom of the conduction band of silicon, due to the Coulomb attraction of electrons to the heteroboundary, considered earlier for interband transitions in nanoisland structures.

Carbon is known to have a smaller lattice parameter than silicon. In principle, this permits us to compensate for the elastic deformation arising from the difference between the lattice parameters of silicon and germanium and even completely suppress the lattice stresses, provided the empirical relation $x = 8.3y$ is satisfied in the $\text{Si}_{1-x-y}\text{Ge}_x\text{C}_y$ alloy [17].

Coming back to the mechanism of spontaneous nanoisland formation, it is worthwhile to note that carbon involvement in the growth process makes it possible to control island size, i.e., reduce it to a few nanometers, when it is essential to quantize the electronic spectrum in all three spatial directions. A great variety of such structures have recently been grown and investigated in different laboratories [18].

5. Conclusion

Results of theoretical and experimental studies reported in the present paper suggest new possibilities for the application of self-assembled GeSi nanoislands and $\text{Si}_{1-x-y}\text{Ge}_x\text{C}_y/\text{Si}$ heterostructures to further improve the efficiency of radiative recombination in silicon-based devices.

The authors are grateful to V Ya Aleshkin, B A Andreev, N A Bekin, N A Vostokov, I V Dolgov, Yu N Drozdov, D N Lobanov, V V Postnikov, M V Stepikhova, and D O Filatov who participated in the evaluation of various characteristics of $\text{Si}_{1-x}\text{Ge}_x/\text{Si}$ and $\text{Si}_{1-x-y}\text{Ge}_x\text{C}_y/\text{Si}$ structures and thereby contributed to the progress of this work.

The work was supported by the Russian Foundation for Basic Research (project 99-02-16980), the Russian Academy of Sciences Program in support of young scientists, the BRHE Program (project RESC-02), the Program “Physics of solid-state nanostructures” (project 99-2047), and the Program “Promising technologies and devices for micro- and nano-electronics” of the Ministry of Science and Technology of Russian Federation (project 02.04.1.1.16.E1).

References

1. Aleshkin V Ya et al. *Pis'ma Zh. Eksp. Teor. Fiz.* **67** 46 (1998) [*JETP Lett.* **67** 48 (1998)]
2. Aleshkin V Ya et al. *Izv. Ross. Akad. Nauk, Ser. Fiz.* **63** 301 (1999)
3. Vostokov N V et al. *Fiz. Tekh. Poluprovodn.* **34** 8 (2000) [*Semicond* **34** 6 (2000)]
4. Collins R T, Fauchet P M, Tischler M A *Phys. Today* **50** (1) 24 (1997)
5. Hirschman K D et al. *Nature* (London) **384** 338 (1996)
6. Coffa S, Franzo G, Priolo F *MRS Bull.* **23** (4) 25 (1998)
7. Andreev A Yu et al. *J. Cryst. Growth* **201/202** 534 (1999)
8. Zhao X et al. *Appl. Phys. Lett.* **74** 120 (1999)
9. Cirlin G E et al. *Semicond. Sci. Technol.* **13** 1262 (1998)
10. Abstreiter G et al. *Semicond. Sci. Technol.* **11** 1521 (1996)
11. Mo Y M et al. *Phys. Rev. Lett.* **71** 2082 (1990)
12. Ross F M, Tersoff J, Tromp R M *Phys. Rev. Lett.* **80** 984 (1998)
13. Bruner K, Eberl K, Winter W *Phys. Rev. Lett.* **76** 303 (1996)
14. Van de Walle C *Phys. Rev. B* **39** 1871 (1989)
15. Osten H J J. *Appl. Phys.* **84** 2716 (1998)
16. Cardona M, Cristensen N E *Phys. Rev. B* **37** 1011 (1988)
17. Eberl K et al. *Appl. Phys. Lett.* **60** 3033 (1992)
18. Schmidt O G et al. *Thin Solid Films* **336** 248 (1998)